

Flat polymeric microlens array

Hongwen Ren, Yi-Hsin Lin, Shin-Tson Wu *

College of Optics and Photonics, University of Central Florida, 4000 Central Florida Blvd., Orlando, FL 32816, USA

Received 19 September 2005; received in revised form 5 December 2005; accepted 7 December 2005

Abstract

A polymer-based flat microlens array is demonstrated. Within each pixel of the array, the polymer presents a circular central-symmetric inhomogeneous orientation. Pixel with such a structure behaves a lens-like character. A suitable amount of liquid crystal mixed in the polymer host can improve not only the lens flexibility but also the lens performance. Moreover, the polymer-based microlens array has the advantages of real planar surface, ultra-thin thickness, and can be designed with any aperture size.

© 2005 Elsevier B.V. All rights reserved.

Micro lens array is an important optical element for information processing, optoelectronics, optical communications, and three-dimensional (3D) displays. Several methods for fabricating microlens and microlens array using glass [1], polymer [2,3], and liquid crystal (LC) [4–13] have been demonstrated. Among them, the solidified polymeric lens is particularly attractive because of its flexibility, simple fabrication process, and low cost. For example, polymer can be easily molded to any lens shape in its glassy state. Unlike glass materials, a solidified polymer is flexible but not fragile. Different from LC lenses, a solidified polymer can stand alone and does not require any substrates to support. Therefore, the polymeric lens system can be light-weight and ultra-thin. Integrating with a 2D display device, such as a liquid crystal display, the flexible microlens array hold promise for improving the viewing angle [14] and creating 3D effect [15,16].

Similar to a glass lens, a conventional polymer lens belongs to the surface-relief lens category. A lens with surface-relief structure can provide high focal power, however, to decrease the thickness of the polymer lens and the size of the lens aperture is rather difficult and the associated cost is high. A more serious problem is that a polymer microlens cannot be placed inside the LC device due to its surface-relief structure. Usually, the lens system is placed outside

of the LC device. Thus, the lens surface has to be protected from being damaged. In a previous publication [13], we reported a planar lens which was fabricated by using nano-sized polymer-dispersed liquid crystals to fill the sags of the lens instead of air. Essentially, the fabrication method of this planar lens is similar to that of the surface-relief lens. As a result, the above-mentioned problems for the surface-relief lens still exist.

In this paper, we demonstrate a polymer-based microlens which can focus light due to its central-symmetric inhomogeneous gradient index distribution, rather than surface-relief structure. In this microlens, polymers present central-symmetric inhomogeneous orientation similar to that of the LC directors in a LC lens. To prepare a demo, we used patterned hole-electrode to fabricate microlens arrays. Depending upon the size and shape of the hole electrode and the LC cell gap, various planar microlens arrays can be fabricated easily.

Fig. 1 illustrates the fabrication procedures of the proposed polymer lens. The diacrylate monomer we selected exhibits a nematic phase. Therefore, the UV-curable LC diacrylate monomers can be treated with homogeneous alignment, as shown in Fig. 1(a). This is an essential part of the material system. The indium–tin-oxide (ITO) electrode on the upper substrate was etched with circular holes. When a voltage is applied across the LC cell, as Fig. 1(b) depicts, a central-symmetric inhomogeneous electric field is generated near the holes. This electric field induces the

* Corresponding author. Tel.: +1 407 823 4763; fax: +1 407 823 6880.
E-mail address: swu@mail.ucf.edu (S.-T. Wu).

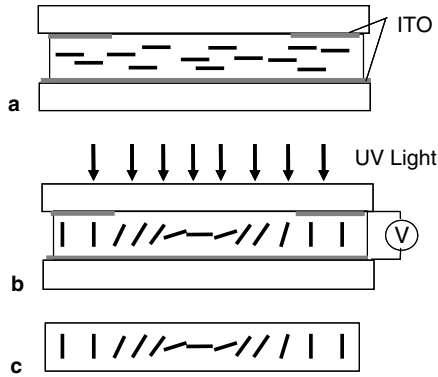
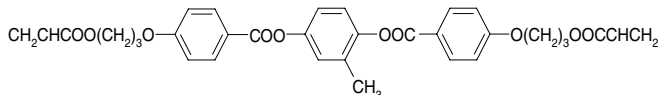


Fig. 1. Procedures for fabricating the polymer microlens. Here, a single pixel is illustrated: (a) homogeneous alignment at $V=0$, (b) central-symmetric inhomogeneous alignment at $V=15 V_{\text{rms}}$ and cured with a UV light, and (c) polymer microlens without substrates. The hole diameter on the top substrate is $140 \mu\text{m}$ and cell gap is $25 \mu\text{m}$.

LC monomers to form a variable central-symmetric profile, as Fig. 1(b) depicts. After UV exposure, the gradient distribution of the LC monomers is fixed. Peeling off the substrates, we obtained a solidified polymeric planar lens, as Fig. 1(c) shows.

The polymeric material system consists of 70 wt% UV curable LC diacrylate monomer (RM-257) and 30 wt% nematic LC E48 (from Merck), whose $n_0 = 1.523$ and birefringence $\Delta n = n_e - n_0 = 0.231$. The mixing of a nematic LC with RM257 leads to several desirable features: (1) it lowers the viscosity of the polymer so that the mixture is easier to be filled into an LC cell, (2) it increases the birefringence of the mixture, and (3) it increases the film's flexibility. RM257 is a rod-like monomer with reactive double bonds at both sides, as shown below:



Similar to a nematic LC, RM257 is a liquid crystal monomer; it exhibits optical and dielectric anisotropies.

Fig. 1 shows the microlens fabrication processes. The LC/monomer mixture was injected to a homogeneous cell in the isotropic state. The inner surfaces of the ITO glass substrates were overcoated with a thin polyimide layer and buffed in antiparallel directions. The top ITO electrode was etched with hole-array. Fig. 1(a) zooms in the single hole structure. The aperture of each hole is $140 \mu\text{m}$ and the cell gap is $25 \mu\text{m}$. After the cell was cooled to room temperature for a few minutes, the LC/monomer mixture presents a stable homogeneous alignment. We observed the cell using a polarized optical microscope. The magnification of the objective lens is $10\times$. The rubbing direction of the cell was oriented at 45° with respect to the axis of the linear polarizer, and the analyzer was crossed. To observe the image clearly, a green color filter ($\lambda = 546 \text{ nm}$) was placed between the analyzer and the light source.

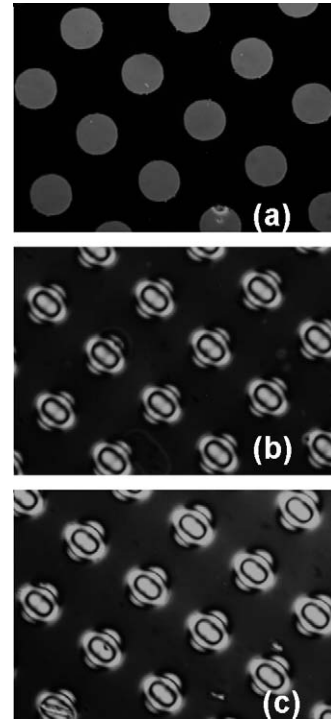


Fig. 2. Interference fringe patterns observed under a polarized optical microscope: (a) $V=0$, (b) $V=15 V_{\text{rms}}$ and cured using a UV light, and (c) $V=0$.

In the voltage-off state, the E48/RM-257 LC/monomer mixture presents a homogeneous alignment. Thus, the transmitted light has a uniform green color, as shown in Fig. 2(a). When a voltage is applied across the cell, a central-symmetric inhomogeneous electric field occurs in the patterned hole-electrodes. The LC diacrylate monomers and LC molecules are reoriented along the electric field direction and their tilt angle is dependent upon the electric field strength. Therefore, a gradient-index profile is obtained within the patterned hole areas. Under such a circumstance, each hole behaves as a lens. Because the lens is polarization dependent, the observed fringes for the light parallel to the rubbing direction (e-fringes) is much more than that for the light perpendicular to the rubbing direction (o-fringes). From Fig. 2(b), the observed elliptical fringes are the combination of e- and o-fringes. If the rubbing direction is parallel or perpendicular to the optical axis of the polarizer, the observed fringes are perfectly circular.

Although the LC/monomer is cured by a UV light, the profile of the gradient-index can still be tuned by changing the applied voltage because of the LC contents. The switching voltage should be quite high because of the high ($\sim 70 \text{ wt}\%$) monomer concentration.

Fig. 2(b) shows a microscope photo of the uncured LC/monomer microlens under a bias voltage $V=15 V_{\text{rms}}$. The interference fringes indicate that a gradient index profile has occurred within the hole. When the cell was illuminated by a UV light, photo-polymerization took place immediately in the LC/monomer mixture and the interference fringes were fixed quickly. When the applied voltage is

removed, the interference rings stay. Cleaving the cell, a thin but solidified polymer film was obtained. Fig. 2(c) shows the microscope image of the polymeric film. The interference rings of the film are as good as those within the cell before cleaving.

To inspect the optical quality of the microlens array, we observed its imaging property under a polarized optical microscope. A small letter “R” which serves as the object was placed below the analyzer. By tuning the distance between the ocular (5×) and the sample, multiple images of the object through the microlens arrays were clearly observed, as shown in Fig. 3. The clear images imply that the peeling of substrates makes a very negligible effect on the microlens array performance.

The focal length of each microlens in the array can also be measured using the polarized optical microscope. We initially set focus on the microlens surface in order to get clear interference rings. Then, we adjusted the distance between the sample and the ocular in one direction until a clear image was observed, as shown in Fig. 3. The distance traveled is the focal length of the lens. The distance was measured to be ~ 2.3 mm.

From Fig. 2(c), we can estimate the focal length of the microlens array using Fresnel’s approximation [17]:

$$f = \frac{\pi r^2}{\Delta\phi\lambda}, \quad (1)$$

where r is the radius of the microlens, λ is the incident light wavelength, and $\Delta\phi$ is the phase difference between the center and edges of the hole. From Fig. 2(c), there are two interference rings within each hole. Thus, $\Delta\phi \sim 4\pi$ because the phase difference between the neighboring rings is 2π . Knowing the wavelength $\lambda = 546$ nm and the lens radius $r = 70$ μm , we find from Eq. (1) that $f \sim 2.24$ mm. This calculated focal length is almost the same as that we measured using microscope.

The focal length of the microlens can be controlled by the applied voltage before UV exposure, as shown in Fig. 1(b). From Eq. (1), the shortest focal length can be obtained when $\Delta\phi$ reaches its maximum. The phase difference is related to the cell condition as:

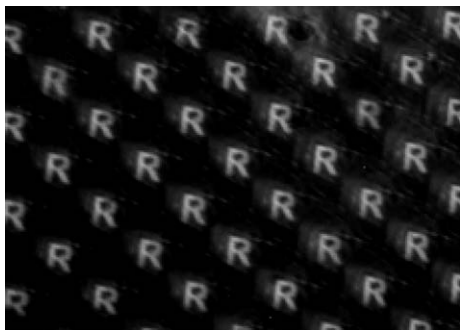


Fig. 3. Microscope imaging properties of the flexible polymer-based planar microlens array. $\lambda = 546$ nm.

$$\Delta\phi = \frac{2\pi d\Delta n}{\lambda}, \quad (2)$$

where d is the cell gap and Δn is the birefringence of the LC mixture. Plugging Eq. (2) into Eq. (1), we find $f = r^2/d\Delta n$. Thus, in order to obtain the shortest focal length by utilizing the maximum birefringence, the ratio of the lens aperture to the cell gap should be optimized. Due to the relatively high viscosity at room temperature, the E48/RM257 LC/monomer mixture responds to the applied electric field very slowly. It is better to control the LC/monomer at a temperature slightly below its clearing point before UV exposure. In our experiment, we cured the E48/RM257 mixture at ~ 80 °C.

Similar to a conventional tunable LC lens, the focal length of the polymer microlens can be tuned by the applied voltage as well because of the embedded 30 wt% LC. To investigate this tunable focus property, the flat polymer film was tightly sandwiched between two ITO glass substrates. The ITO electrode on each substrate is continuous in order to generate a homogeneous electric field across the film. During experiment, the film was fixed without any movement. A collimated He–Ne laser beam ($\lambda = 633$ nm) was used to illuminate the polymeric film. The incident polarization is parallel to the rubbing direction of the film. The transmitted light in the imaging plane was detected by a CCD camera.

Fig. 4(a) and (b) show the intensity profiles of four microlenses at $V = 0$ and 190 V_{rms}, respectively. At $V = 0$, the average focus intensity (at the CCD focal plane) of each microlens exceeds 15,000 arbitrary units. At $V = 190$ V_{rms}, the intensity of each peak decreases slightly. However, the

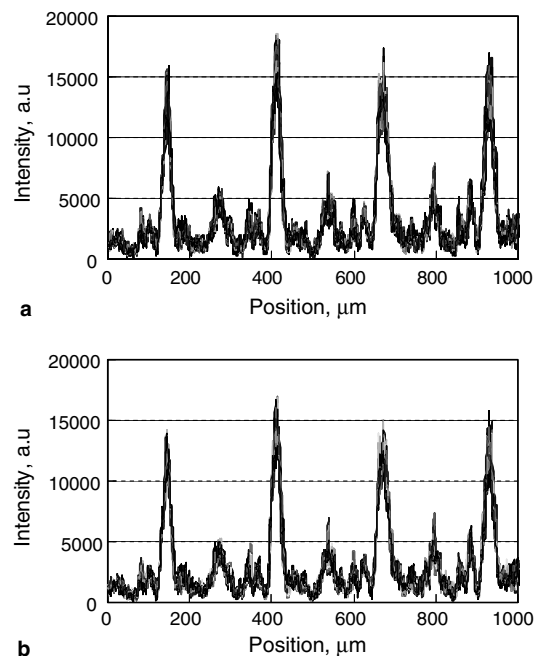


Fig. 4. Intensity profiles of the polymer microlens array recorded by the CCD camera at: (a) $V = 0$, and (b) $V = 190$ V_{rms}. Film thickness $d = 25$ μm and $\lambda = 633$ nm.

beam profile remains the same. This indicates that the reduced intensity is due to focal length change, rather than from the electric-field-induced distortion. The observed high operating voltage originates from two reasons: high polymer concentration and a relatively thick polymer film. The relatively small focus change results from the low LC content. Because of the high polymer concentration, the response time is in the submillisecond range during focus change. To lower the operating voltage, we could increase the LC concentration (up to 70%) without softening the film. The increased LC concentration will also widen the tunable range of the focal length. Another method is to reduce the thickness of the polymeric film. However, reducing the film thickness would lead to a longer focal length, as described in Eq. (1). To compensate for the reduced phase of a thinner film, a high birefringence LC mixture could be considered [18].

In comparison to a conventional polymer microlens array, the major advantages of our polymeric microlens array are flat, ultra-thin, and good flexibility. Moreover, the fabrication procedures are relatively simple. Using an optimized hole-electrode [11] or flat-spherical electrode method [12], polymer microlens arrays can be fabricated easily with arbitrary aperture size and film thickness. Such a polymer-based microlens array can be easily integrated into a LC display device because the lens array can be placed either inside or outside of the display panel. Also, the polymer-based microlens array are found to be useful in organic light-emitting device for improving its light extraction efficiency [19]. By designing a proper electrode structure, various planar optical devices, such as prism grating and Fresnel lens can be fabricated.

In conclusion, we fabricated a polymeric film with microlens array patterns. The size of lens aperture and film thickness can be changed depending upon the shape and size of the designated electrode and the cell gap. Adding a suitable amount of nematic LC in polymer host can improve the microlens performances. The focal length of the microlens

is tunable electrically with very fast response time. Due to real planar, ultra-thin, and flexible, applications of such polymer microlens arrays for 3D displays, improving viewing angle, and improving light efficiency are foreseeable.

Acknowledgments

The authors thank Dr. Sebastian Gauza for his technical assistance and useful discussions.

References

- [1] M. Fritze, M.B. Stern, P.W. Wyatt, *Opt. Lett.* 23 (1998) 141.
- [2] T. Okamoto, M. Mori, T. Karasawa, S. Hayakawa, I. Seo, H. Sato, *Appl. Opt.* 38 (1999) 2991.
- [3] D.M. Hartmann, O. Kibar, S.C. Esener, *Appl. Opt.* 40 (2001) 2736.
- [4] T. Nose, S. Sato, *Liq. Cryst.* 5 (1989) 1425.
- [5] J.S. Patel, K. Rastani, *Opt. Lett.* 16 (1991) 532.
- [6] N.A. Riza, M.C. DeJule, *Opt. Lett.* 19 (1994) 1013.
- [7] A.F. Naumov, G.D. Love, M. Yu Loktev, F.L. Vladimirov, *Opt. Express* 4 (1999) 344.
- [8] L.G. Commander, S.E. Day, D.R. Selviah, *Opt. Commun.* 177 (2000) 157.
- [9] T. Kyu, D. Nwabunma, *Macromolecules* 34 (2001) 9168.
- [10] B. Wang, M. Ye, M. Honma, T. Nose, S. Sato, *Jpn. J. Appl. Phys. Part 2* 41 (2002) L1232.
- [11] S. Masuda, S. Fujioka, M. Honma, T. Nose, S. Sato, *Jpn. J. Appl. Phys* 35 (1996) 4668.
- [12] H. Ren, Y.H. Fan, S. Gauza, S.T. Wu, *Appl. Phys. Lett.* 84 (2004) 4789.
- [13] H. Ren, Y.H. Fan, Y.H. Lin, S.T. Wu, *Opt. Commun.* 247 (2005) 101.
- [14] Y. Kim, J.H. Park, H. Choi, S. Jung, S.W. Min, B. Lee, *Opt. Express* 12 (2004) 421.
- [15] W.L. Ijzerman, S.T. de Zwart, T. Dekker, *SID Tech. Digest* 34 (2005) 98.
- [16] B. Lee, S. Jung, S.W. Min, J.H. Park, *Opt. Lett.* 26 (2001) 1481.
- [17] J.W. Goodman, *Introduction to Fourier Optics*, McGraw-Hill, New York, 1996.
- [18] S. Gauza, H. Wang, C.H. Wen, S.T. Wu, A.J. Seed, R. Dabrowski, *Jpn. J. Appl. Phys. Part 1* 42 (2003) 3463.
- [19] C.F. Madigan, M.H. Lu, J.C. Sturm, *Appl. Phys. Lett.* 76 (2000) 1650.